2. DP AND DS INTERFERENCE

This section provides DTV susceptibility test results and characterization measurements for DP and DS interference.

2.1. Pulse Parameters

DP and DS signals achieve their ultra-wide bandwidth by transmitting pulses of short duration. These signals are specified by pulse width (w), the nominal pulse period (T_{pulse} = 1/PRF, where PRF is the pulse repetition frequency), and fractional dither (f_D) to quantify pulse offset from T_{pulse}. Table 1 specifies parameters that define the DP signals considered in this report. Fractional on-time is approximated as $\zeta \approx w/T_{pulse}$. Figure 1 illustrates pulse parameters for DP-04.

Table 1. DP Pulse Parameters

Type	Index	w (ns)	T_{pulse} (ns)	ζ	f_D
DP	01	0.094	10,000	9.4×10^{-6}	0.5
	02		1000	9.4×10^{-5}	
	03		100	9.4×10^{-4}	
	04		10	9.4×10^{-3}	

Table 2 specifies parameters that define the DS signals considered in this report. Recall that DS devices multiply each data bit by a code word consisting of L chips. The chips have values of {-1, 0, 1} and are transmitted every $T_{chip} = 1/f_{chip}$, where f_{chip} = 1320 million chips per second. The coded data phase modulates pulses that are approximately 0.58 ns wide. Sparse codes used for DS-02, DS-03, and DS-05 are all zeros except for a single one, which results in distinct pulses every $T_{pulse} = LT_{chip}$. DS codes used for DS-04 and DS-06 have relatively few zeros, which results in tightly-packed pulses every $T_{pulse} = T_{chip}$. Figure 2 illustrates pulse parameters for DS-03 and DS-04.

Table 2. DS Pulse Parameters[†]

Type	Index	DS Parameters		Pulse Parameters			
		L	Code Type	w (ns)	T_{pulse} (ns)	ζ	f_D
DS	01	1	N/A	0.58	0.758	0.77	0.0
	02	3	Sparse		2.27	0.26	
	03	6	Sparse		4.55	0.13	
	04	12	DS		0.758	0.77	
	05	12	Sparse		9.09	0.064	
	06	24	DS		0.758	0.77	

[†] The specific codes are [1] for DS-01, [0 1 0] for DS-02, [0 0 1 0 0 0] for DS-03, [0 -1 -1 -1 1 1 1 -1 1 1 -1 1] for DS-04, [0 0 0 0 0 0 0 0 1 0 0 0] for DS-05, and [-1 1 -1 -1 1 -1 -1 1 -1 0 -1 0 -1 -1 1 1 1 -1 1 1 1 -1 -1 -1] for DS-06.

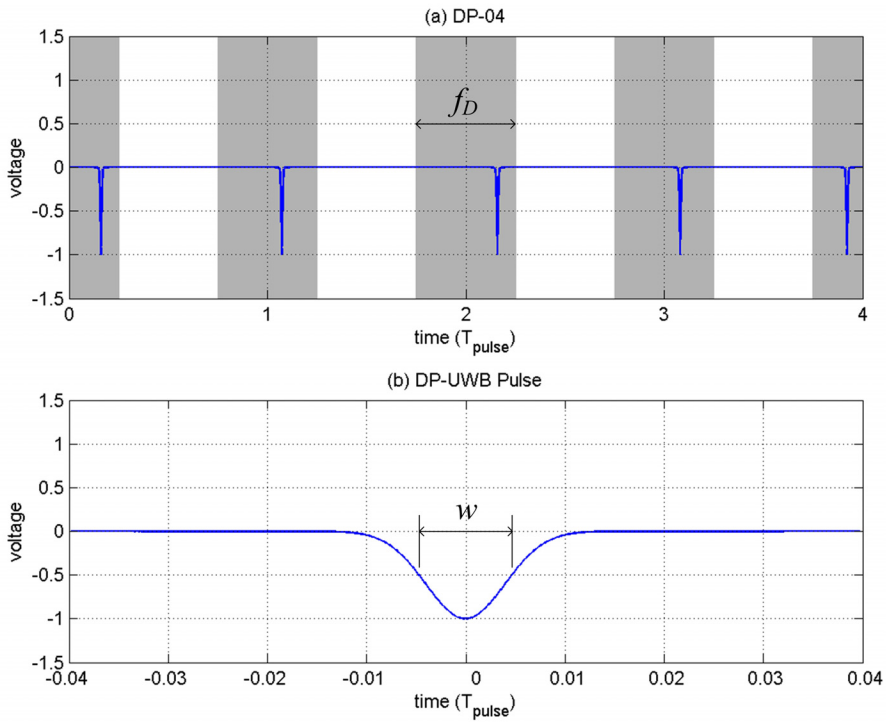

Figure 1. Simulated DP-04 (T_{pulse} = 10 ns).

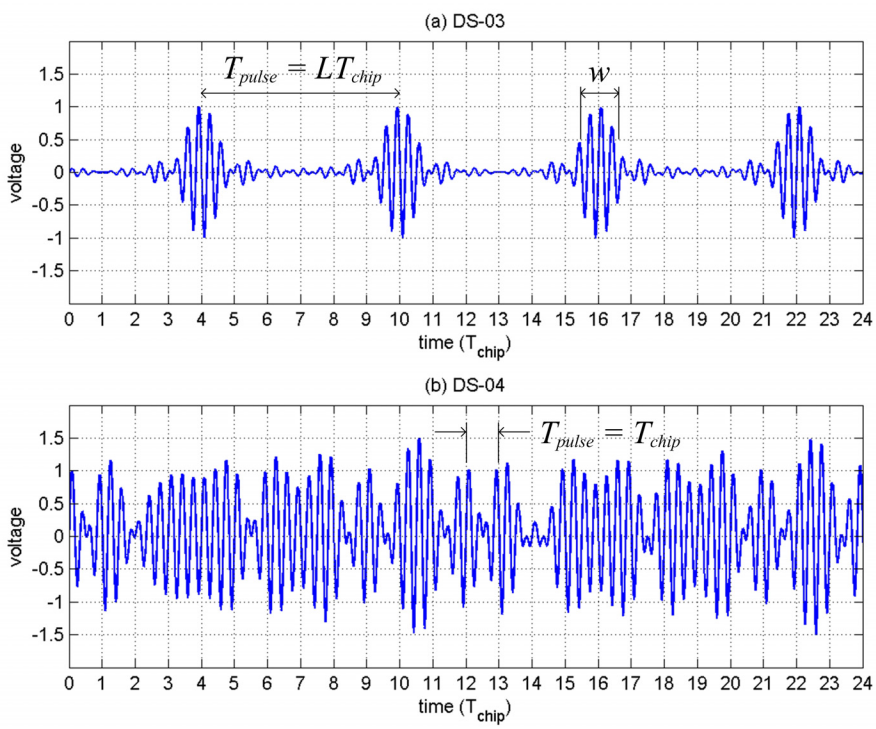

Figure 2. Simulated (a) DS-03 and (b) DS-04 transmitting random data (T_{chip} = 0.758 ns).

2.2. DTV Susceptibility to DP and DS Interference

Results of the DTV susceptibility tests for DP and DS interference are described in this section. Post-Reed-Solomon segment error rate and pre-Viterbi bit error rate are plotted versus the ratio of average interference power to average noise power. Additionally, DTV susceptibility and FEC performance metrics, i.e., INR_{TOV} and BER_{TOV}, are plotted versus $1/\zeta$ in dB. Figure 3 illustrates reference points for signal powers and DTV signal quality metrics acquired during the DTV susceptibility tests.

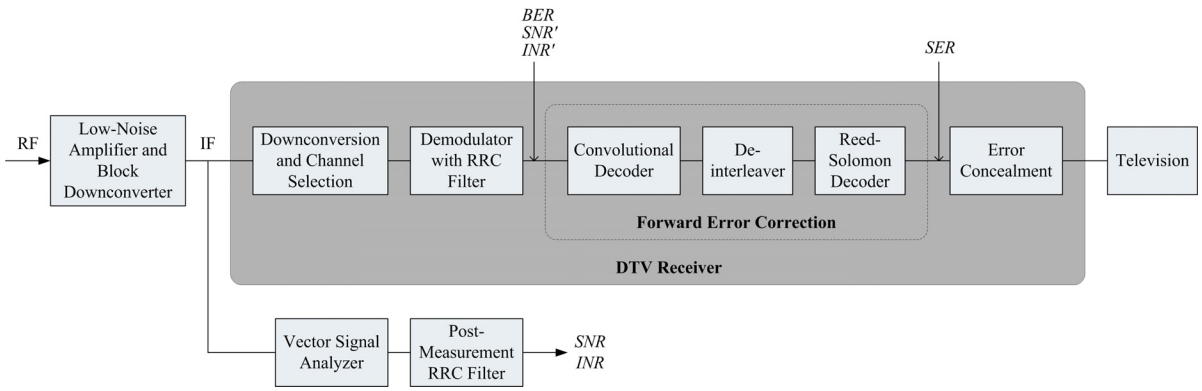

Figure 3. *SNR*, *SNR'*, *INR*, *INR'*, *BER*, and *SER* reference points.

2.2.1. DTV Signal Quality as a Function of Interference Average Power

Figures 4 – 9 provide composite plots of measured *SER* and *BER* as a function of *INR* for measured *SNR* = {9, 12, 15} dB corresponding to *SNR'* = {8.2, 10.5, 12.5} dB at the output of the demodulator. Each page is dedicated to a single *SNR*, each plot is dedicated to a specific signal type, and each curve represents a single T_{pulse}. Figures 4, 6, and 8 provide composite plots of *SER*, while Figures 5, 7, and 9 provide composite plots of *BER*. For each plot, Gaussian noise (GN-01) results are provided as a reference.

The following are general comments regarding the shift, separation, and slope of these *SER* and *BER* curves. Both *BER* and *SER* shifted toward greater *INR* with increasing *SNR*. This occurred because more interference was needed to degrade stronger satellite signals. The shift of DP-01 *BER* and *SER* was significantly greater than the other interference signals. *SER* due to DS signals was similar to *SER* due to GN-01. *SER* due to DP signals showed separation from GN-01 only when T_{pulse} was greater than 100 ns. Relative to Gaussian-noise degradation, the DTV receiver was more susceptible to DP-02 and less susceptible to DP-01. With the exception of DP-01 and DP-02, all DP and DS *SER* curves were steeper than corresponding *BER* curves, which indicates that *SER* was more sensitive than *BER* to changes in average interference power as expected with forward error correction. When $T_{pulse} > 100$ ns, the *SER* slope flattened with increasing T_{pulse}. In fact, the slope of DP-01 *SER* was so low that oscillations indicative of the systematic error mentioned in Appendix B of Part 2 of this report series were revealed.

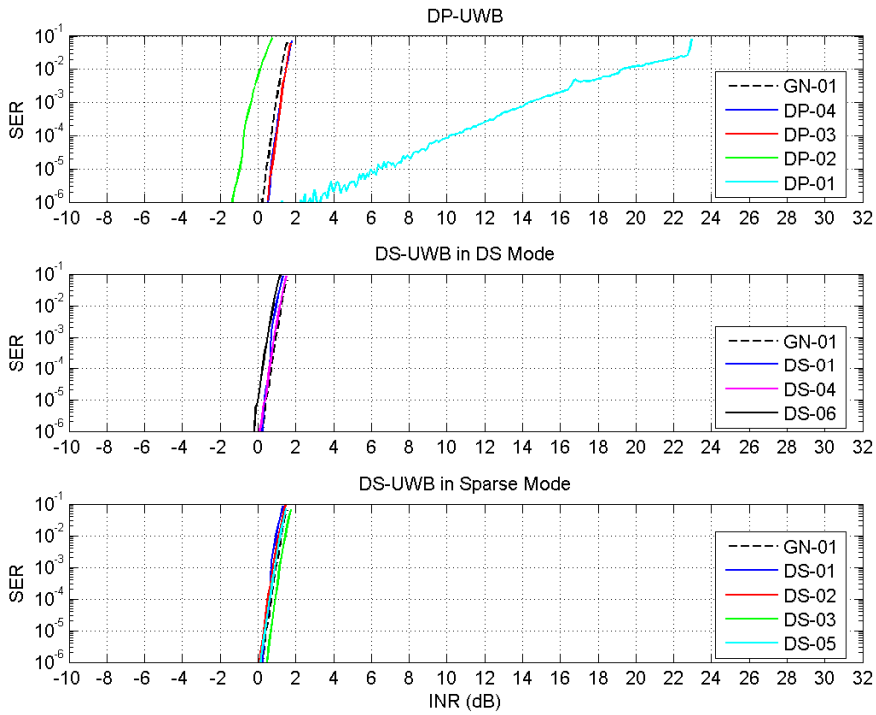

Figure 4. *SER* versus *INR* for a DTV channel operating at *SNR* = 9 dB and exposed to DP and DS interference.

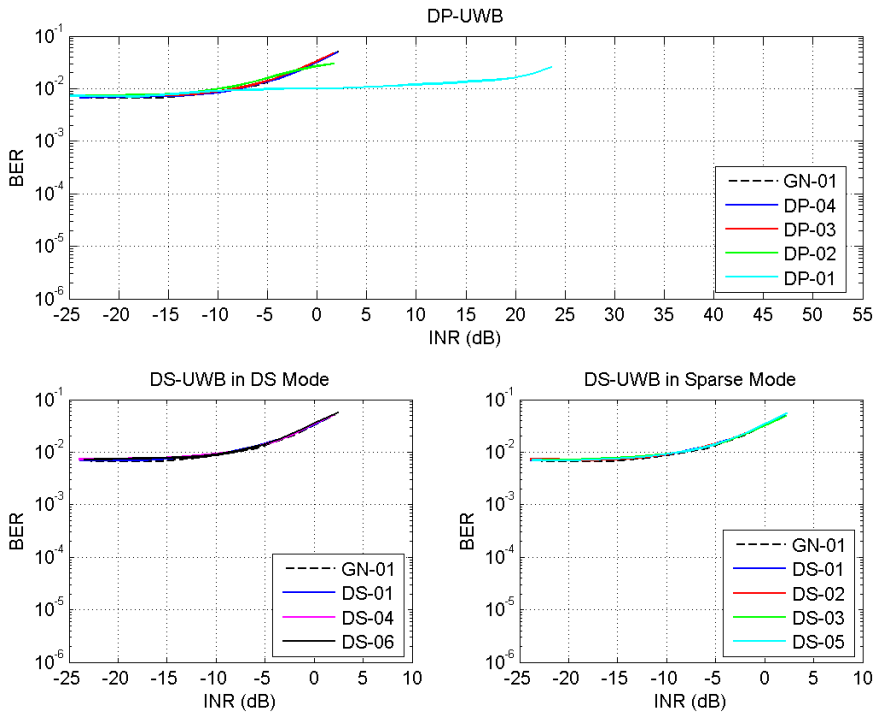

Figure 5. *BER* versus *INR* for a DTV channel operating at *SNR* = 9 dB and exposed to DP and DS interference.

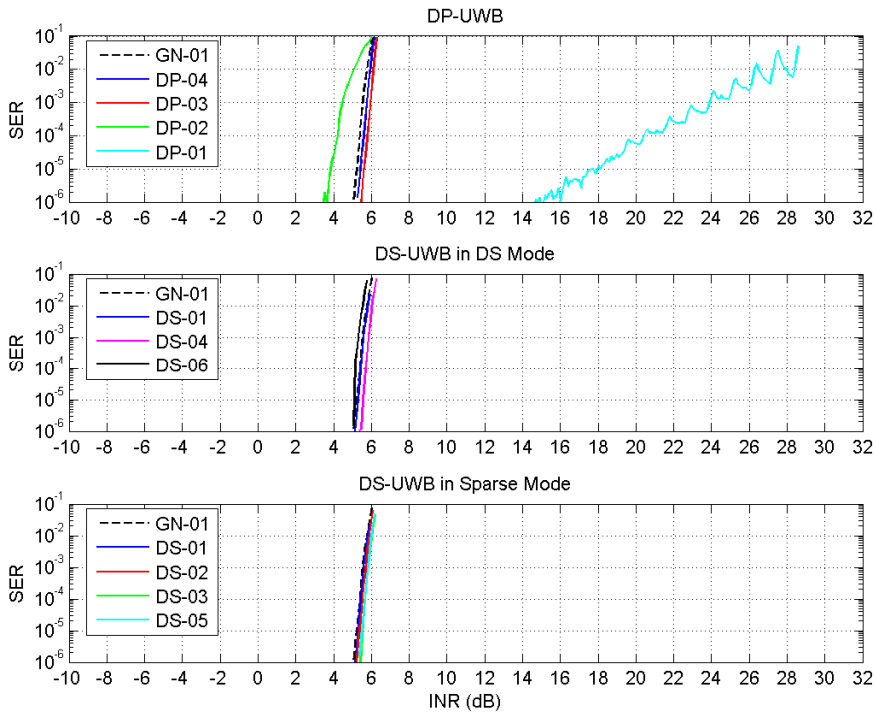

Figure 6. *SER* versus *INR* for a DTV channel operating at *SNR* = 12 dB and exposed to DP and DS interference.

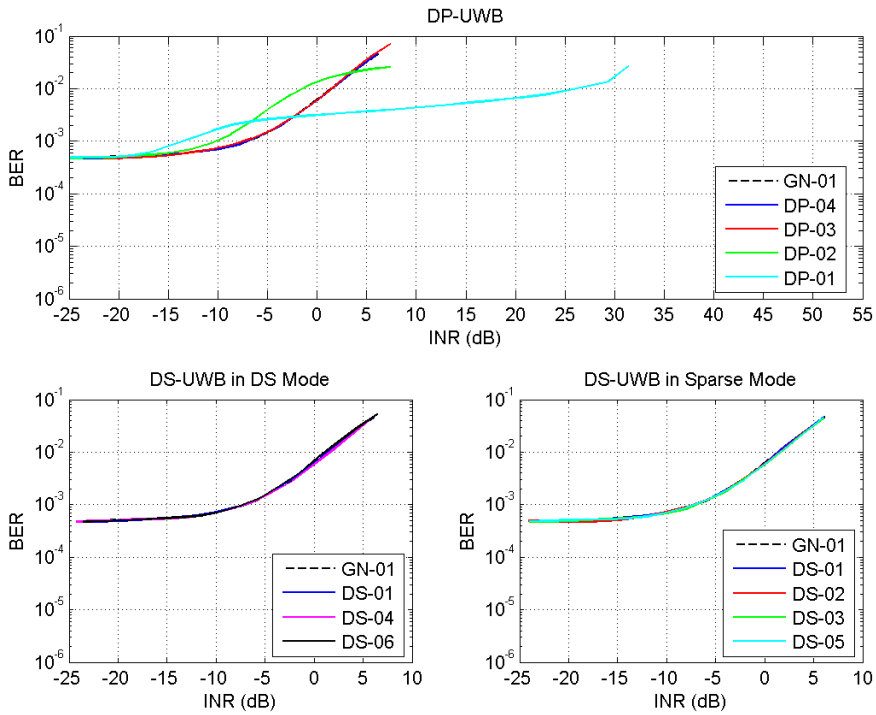

Figure 7. *BER* versus *INR* for a DTV channel operating at *SNR* = 12 dB and exposed to DP and DS interference.

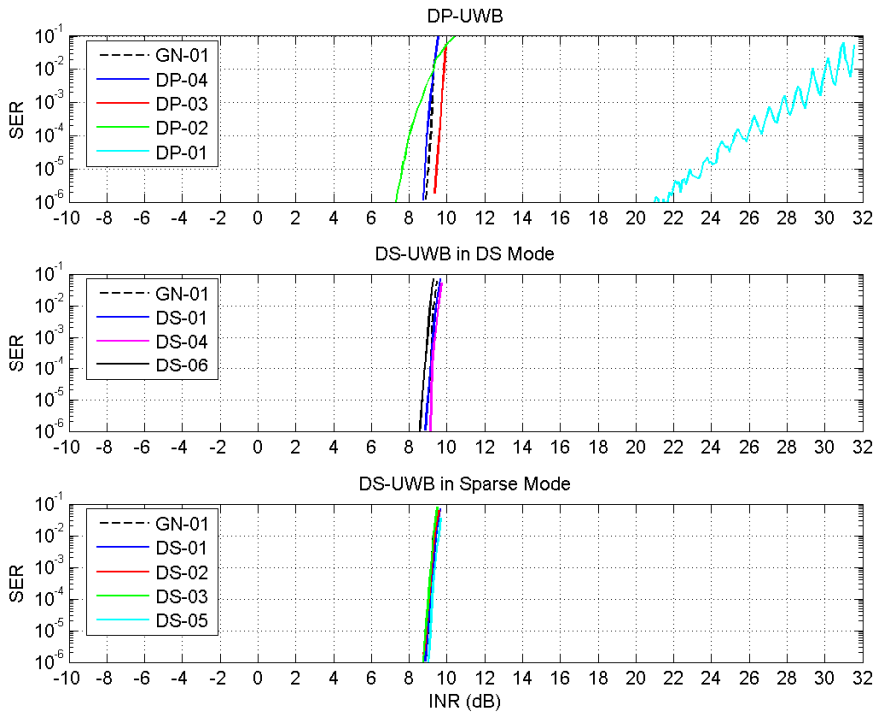

Figure 8. *SER* versus *INR* for a DTV channel operating at *SNR* = 15 dB and exposed to DP and DS interference.

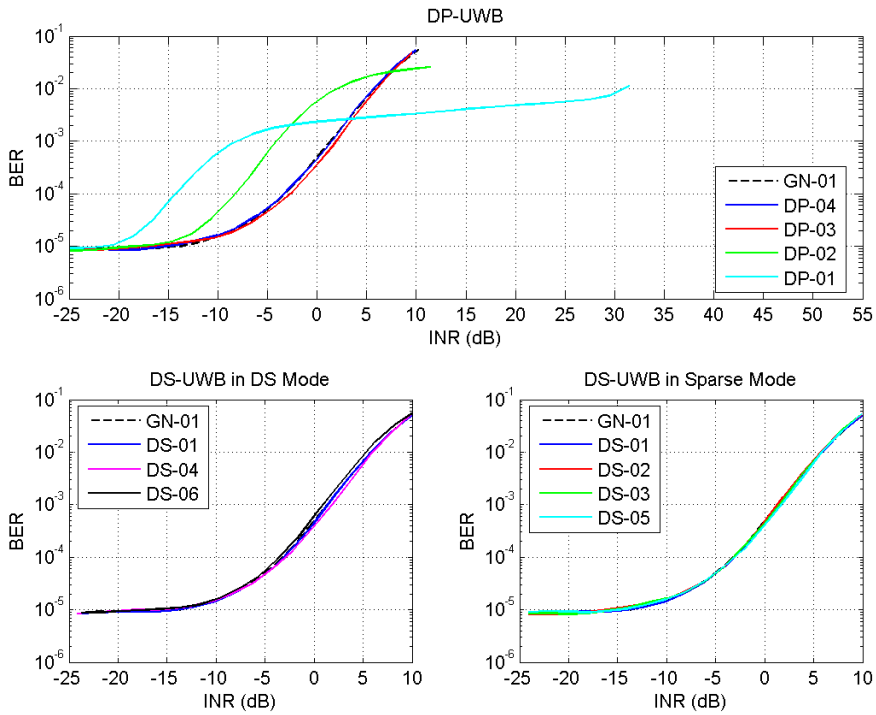

Figure 9. *BER* versus *INR* for a DTV channel operating at *SNR* = 15 dB and exposed to DP and DS interference.

2.2.2. DTV Susceptibility as a Function of Fractional On-Time

Figure 10 displays measured *SER* and *BER* curves for a DTV victim receiver operating at *SNR* = 15 dB and exposed to increasing levels of Gaussian noise interference. This figure also identifies important DTV susceptibility and FEC performance metrics. Importantly, $SER_{TOV} = 10^{-4}$ is a level identified by video quality studies [8] as the threshold of visibility (TOV) where video quality degradation is first evident.

The *INR* that corresponds to SER_{TOV}, INR_{TOV}, is our primary DTV susceptibility metric. That is, receiver susceptibility increases as INR_{TOV} decreases. The *BER* that corresponds to SER_{TOV}, BER_{TOV}, is our FEC performance metric. This metric quantifies the ability of the FEC to overcome bit errors caused by interference to achieve SER_{TOV}. In other words, larger BER_{TOV} indicates more corrected bits and better FEC performance at the threshold of visibility.

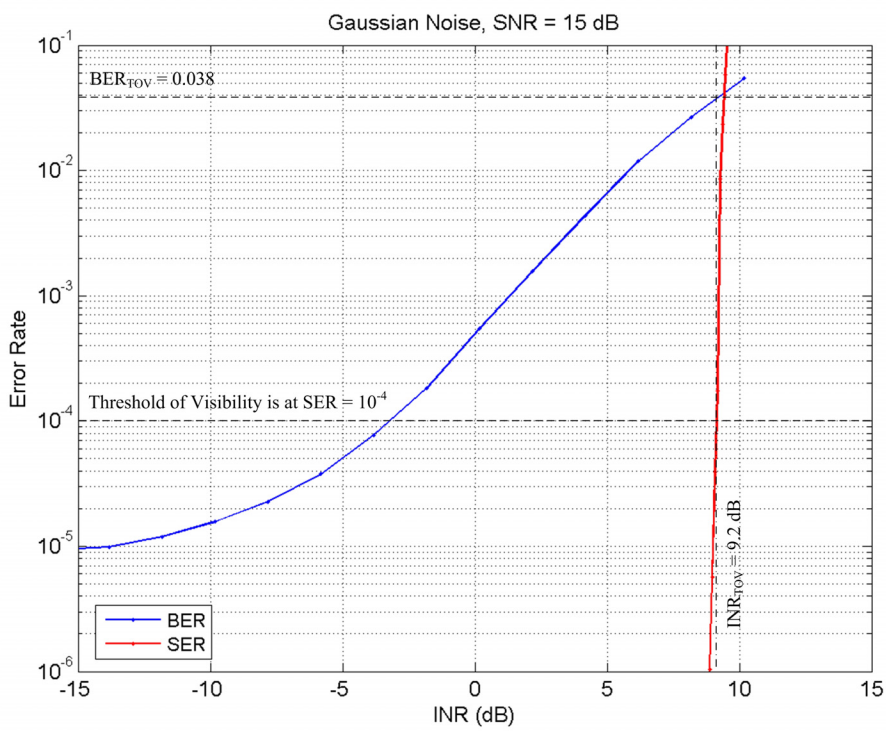

Figure 10. Illustration of threshold-of-visibility metrics.

Table 3 gives INR_{TOV} and BER_{TOV} results for DP and DS interference; GN-01 results from Part 2 of this report series are also included for comparison purposes. Differences between INR_{TOV} of DS, DP-03, DP-04, and GN-01 results were less than 0.5 dB.

Table 3. Measured DTV Susceptibility and FEC Performance for DP and DS Interference

Type	Index	$SNR \approx$ 9 dB		$SNR \approx$ 12 dB		$SNR \approx$ 15 dB	
		INR_{TOV} (dB)	BER_{TOV}	INR_{TOV} (dB)	BER_{TOV}	INR_{TOV} (dB)	BER_{TOV}
DP	01	10.2	0.012	20.4	0.007	25.2	0.006
	02	-0.7	0.025	4.2	0.021	8.0	0.022
	03	1.0	0.041	5.8	0.045	9.6	0.049
	04	0.9	0.038	5.6	0.039	9.0	0.040
DS	01	0.6	0.038	5.4	0.038	9.1	0.038
	02	0.5	0.038	5.5	0.038	9.1	0.039
	03	0.9	0.038	5.7	0.039	9.0	0.040
	04	0.6	0.039	5.7	0.041	9.2	0.042
	05	0.6	0.039	5.7	0.041	9.2	0.042
	06	0.2	0.037	5.2	0.038	8.8	0.039
GN	01	0.7	0.038	5.4	0.038	9.2	0.038

Recall from Part 2 of this report series that high DTV susceptibility, i.e., low INR_{TOV}, correlated with poor FEC performance, i.e., low BER_{TOV}. This demonstrated that DTV susceptibility was related to how effective the FEC was at overcoming bit errors caused by the interference at TOV. DP-01 demonstrates a distinct contrast with this trend, i.e., high DTV susceptibility did not correspond to poor FEC performance based on the chosen metric BER_{TOV}.

Figures 11 – 16 provide plots of INR_{TOV} and BER_{TOV} as a function of $10\log(1/\zeta)$, where DP pulse parameters $w = 0.094$ ns and $T_{pulse} = \{10^4, 10^3, 10^2, 10\}$ ns correspond to $\zeta = \{9.4\times10^{-6}, 9.4\times10^{-5}, 9.4\times10^{-4}, 9.4\times10^{-3}\}$ and $10\log(1/\zeta) = \{50, 40, 30, 20\}$ dB, and DS pulse parameters $w = 0.58$ ns and $T_{pulse} = \{0.758, 2.27, 4.55, 9.09\}$ ns correspond to $\zeta = \{0.77, 0.26, 0.13, 0.064\}$ and $10\log(1/\zeta) = \{1.6, 5.9, 8.9, 12\}$ dB. The independent variable $10\log(1/\zeta)$ was chosen because average power is proportional to ζ. Data points for DS-04 and DS-06 were excluded from the plots because they have the same ζ as DS-01. The horizontal dashed reference line in each INR_{TOV} plot corresponds to DTV susceptibility to Gaussian noise interference. Results demonstrate that DTV susceptibility can be related to particular pulse parameters. Generally speaking, DTV susceptibility to DS interference and DP interference with $10\log(1/\zeta) \leq 30$ dB was comparable to that of Gaussian noise interference. At larger $10\log(1/\zeta)$, however, the DTV receiver was relatively more susceptible to DP-02 and less susceptible to DP-01.

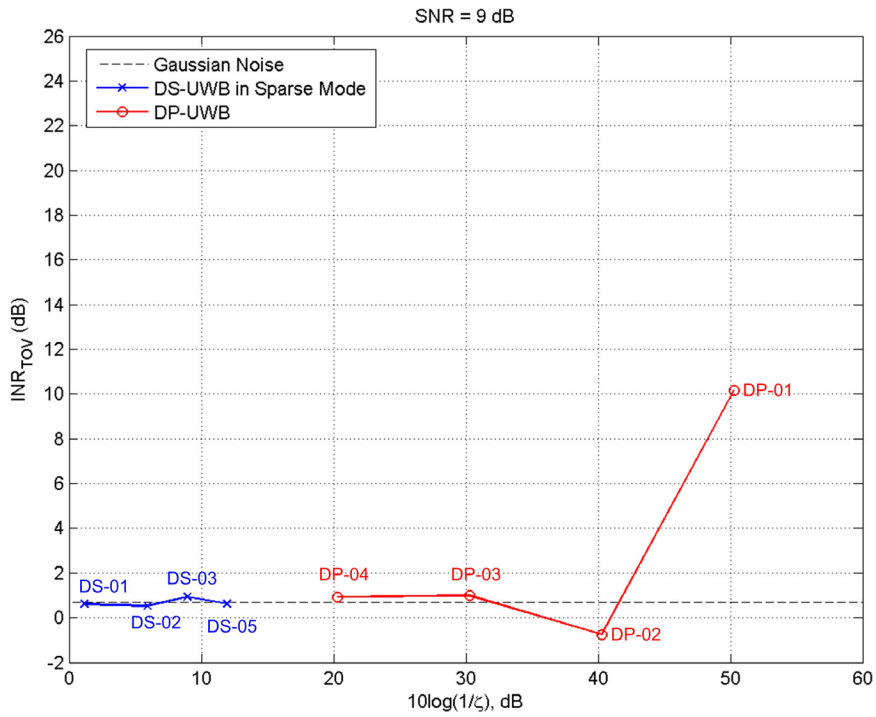

Figure 11. INR_{TOV} versus 10log(1/ζ) for a DTV channel operating at SNR = 9 dB and exposed to DP and DS interference.

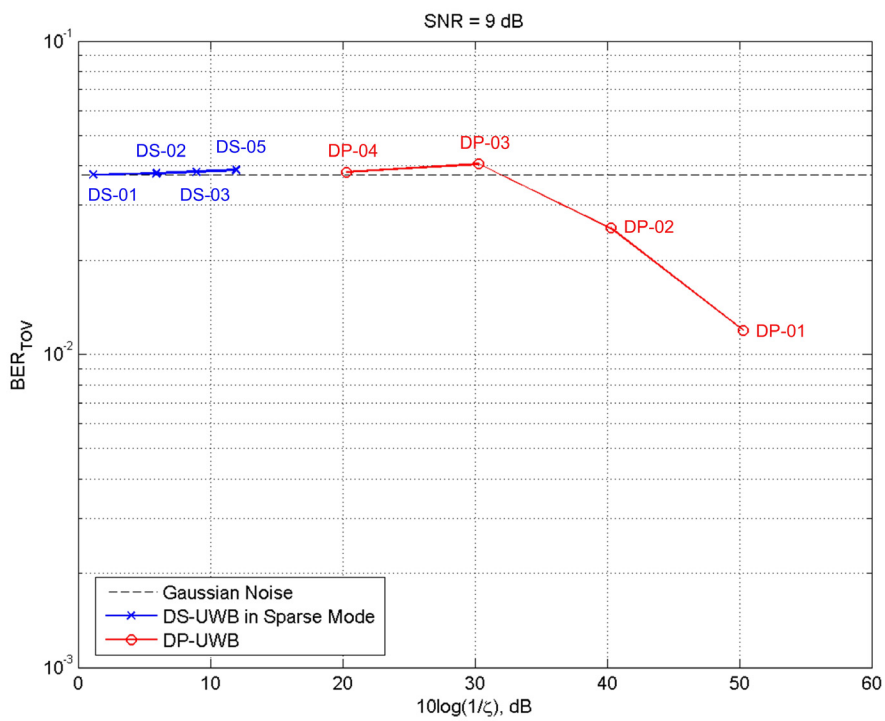

Figure 12. BER_{TOV} versus 10log(1/ζ) for a DTV channel operating at SNR = 9 dB and exposed to DP and DS interference.

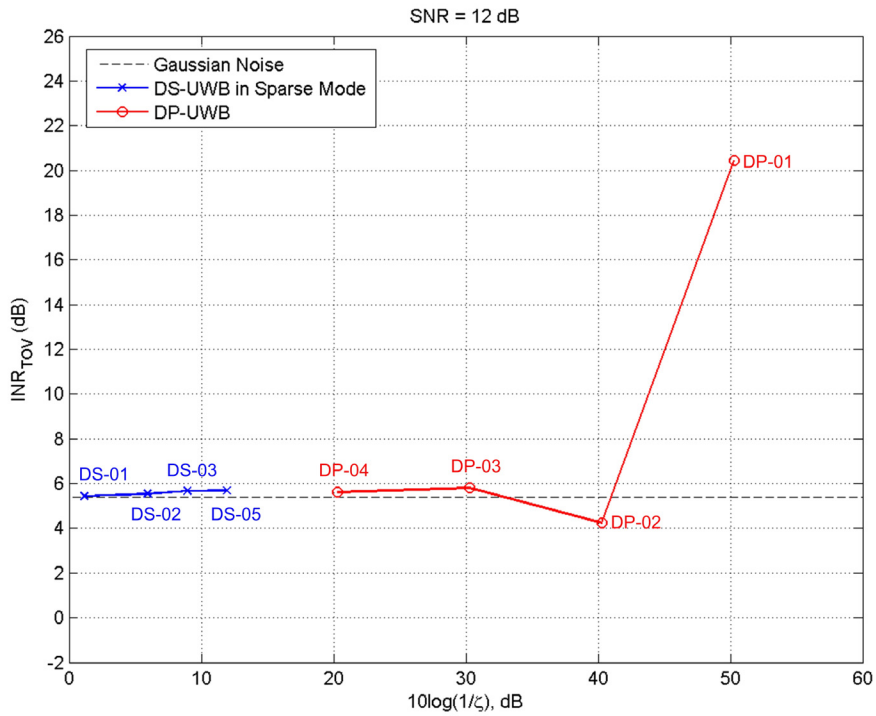

Figure 13. INR_{TOV} versus 10log(1/ζ) for a DTV channel operating at SNR = 12 dB and exposed to DP and DS interference.

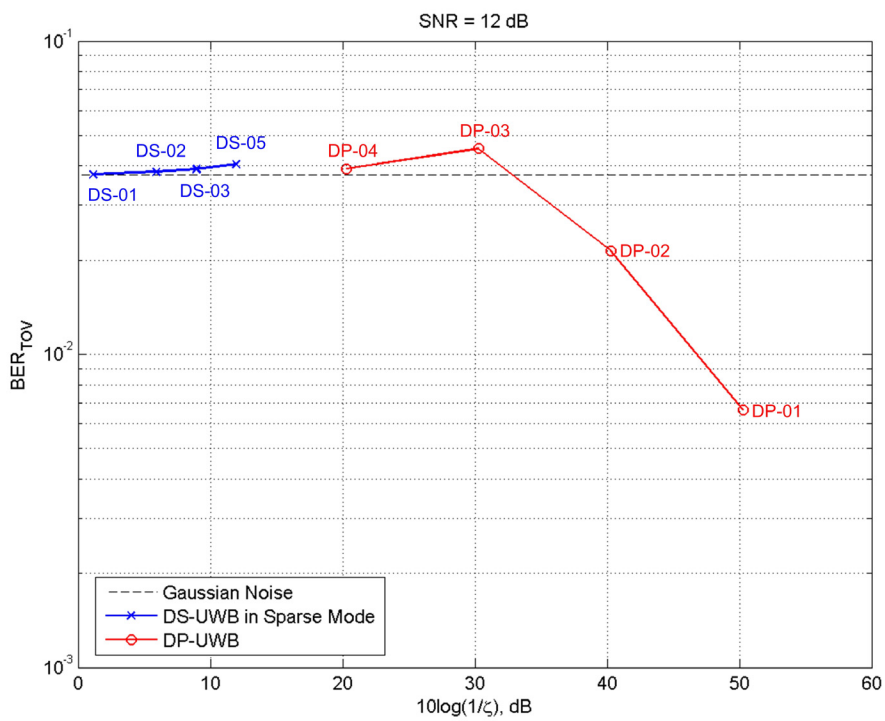

Figure 14. BER_{TOV} versus 10log(1/ζ) for a DTV channel operating at SNR = 12 dB and exposed to DP and DS interference.

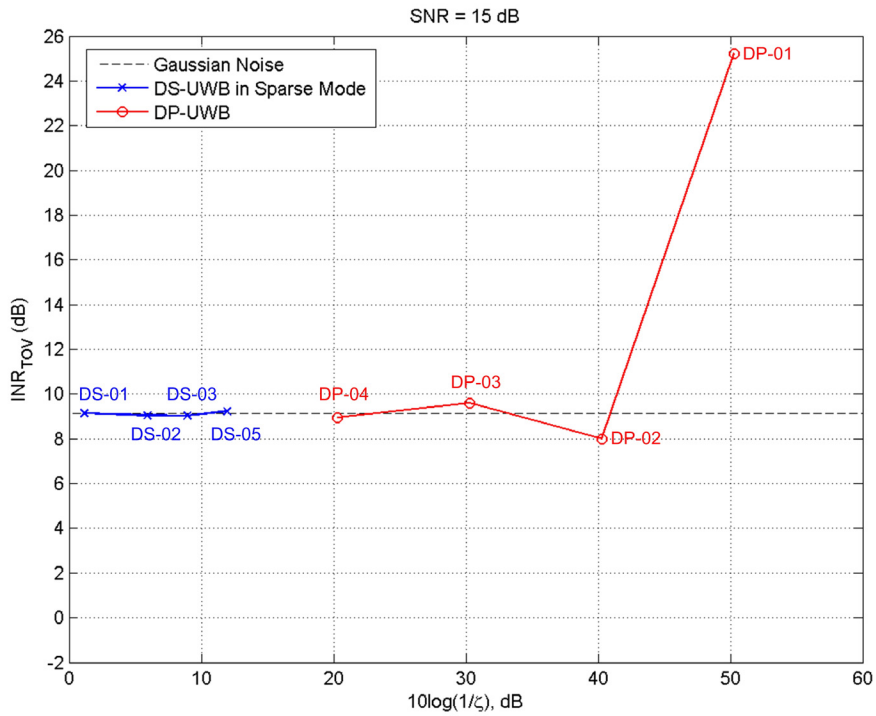

Figure 15. INR_{TOV} versus 10log(1/ζ) for a DTV channel operating at SNR = 15 dB and exposed to DP and DS interference.

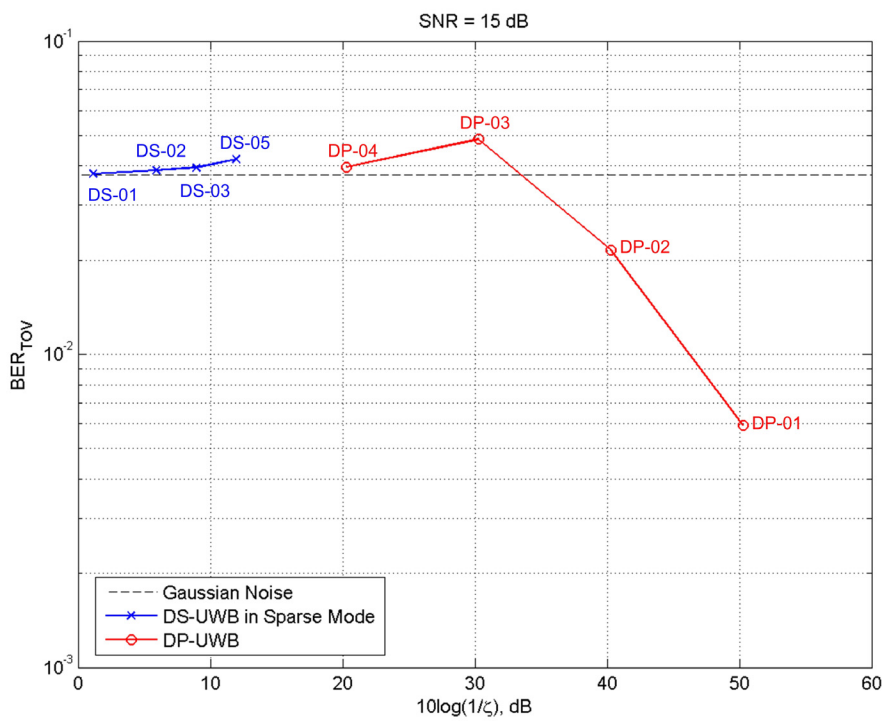

Figure 16. BER_{TOV} versus 10log(1/ζ) for a DTV channel operating at SNR = 15 dB and exposed to DP and DS interference.

2.3. Characterization of DP and DS Signals

Characterization of the DP and DS signals was accomplished via temporal, amplitude, and spectral analyses. The UWB signals were measured with the vector signal analyzer under optimal measurement conditions at the RF output of the vector signal generator. Appendix B discusses the measurement setup and provides an extensive set of results. This section provides band-limited signal characterization results for the B_{DTV} = 19.51-MHz DTV receiver root-raised-cosine (RRC) filter.

2.3.1. Temporal Analysis

Temporal characteristics of the DP and DS signals were evaluated with crossing statistics, i.e., probabilities of the time duration that commences when a signal crosses an amplitude threshold and stays either above or below that threshold. Measured cumulative distribution functions for pulse duration (*PD*) and pulse interval (*PI*) statistics are given in Section B.2. Burst duration (*BD*) and burst interval (*BI*) are defined as the 10th percentile of *PD* and *PI*, respectively, using a crossing threshold equal to -70 dBm. This crossing threshold was useful for quantifying the effects of band-limiting on temporal characteristics of UWB signals, because it is high enough to avoid significant contribution from the measurement system noise floor and low enough to discern pulses and gated signals given the described measurement conditions.

Table 4 summarizes the effects of band-limiting on the temporal characteristics of the DP and DS signals. DP-01 and DP-02 pulses were resolved because T_{pulse} was significantly greater than $1/B_{DTV}$. As expected for these signals, band-limiting lengthened pulse widths, $BD > w$, and increased fractional on-times, $\zeta_{DTV} = BD/(BD + BI) > \zeta$. Notice that *BI* for DP-01 was greater than T_{pulse} due to dithering. *BD* and *BI* are less meaningful estimates when pulses are not resolved in the limiting bandwidth B_{DTV}, because there are no on- and off-times to distinguish. This was the case for DS signals, DP-03, and DP-04, whose crossing statistics resembled those of GN-01, i.e., *BI* was invariably 0.02 µs, and the variability in *BD* had little effect on $\zeta_{DTV} \approx 1$.

Table 4. Measured Temporal Characteristics of DP and DS Signals Band-Limited to B_{DTV}

Type	Index	Pulse Parameters			Band-Limited Metrics		
		w (µs)	T_{pulse} (µs)	ζ	*BD* (µs)	*BI* (µs)	ζ_{DTV}
DP	01	0.000094	10.0	9.4×10^{-6}	0.22	11.24	0.02
	02		1.0	9.4×10^{-5}	0.20	0.91	0.18
	03		0.1	9.4×10^{-4}	2.26	0.02	0.99
	04		0.01	9.4×10^{-3}	8.46	0.02	1.00
DS	01	0.00058	0.000758	0.77	7.40	0.02	1.00
	02		0.00227	0.26	8.36	0.02	1.00
	03		0.00455	0.13	8.10	0.02	1.00
	04		0.000758	0.77	9.03	0.02	1.00
	05		0.00909	0.064	11.22	0.02	1.00
	06		0.000758	0.77	3.71	0.02	0.99
GN	01	N/A	N/A	1.00	6.92	0.02	1.00

2.3.2. Amplitude Analysis

Amplitudes of the DP and DS signals were characterized with amplitude probability distributions, which give the probability that the signal amplitude exceeds a certain value. In this report, *APD*s are plotted on Rayleigh graphs where Rayleigh-distributed amplitudes of complex-Gaussian noise appear as a negatively-sloped, straight line. The sorting method, documented in Appendix D of Part 1 of this report series, was used to estimate and plot *APD*s of 131,072 samples that are free of correlation introduced by the measurement system bandwidth and band-limiting in post-measurement processing.

Figures 17 and 18 provide composite *APD* plots of measured DP and DS signals, respectively. The upper bound of the shaded region is the average power of the VSA noise, approximately -79.7 dBm in B_{DTV}. Notice that measured average powers, indicated in the legends, were proportional to ζ. Band-limiting had profound effects on the *APD*s of the DP and DS signals. For signals with $T_{pulse} > 1/B_{DTV}$, a step-like *APD* occurred, where higher amplitudes corresponded to elongated pulses and lower amplitudes corresponded to system noise observable during the shortened off-times between pulses. DP-01 and DP-02 band-limited to B_{DTV} have step-like *APD*s. For signals with $T_{pulse} \leq 1/B_{DTV}$ a negatively-sloped, straight *APD* can occur, corresponding to Rayleigh-distributed amplitudes due to elongated pulses overlapping each other. DS-01 and DS-02 band-limited to B_{DTV} have Rayleigh-distributed *APD*s.

Table 5 summarizes measured peak-to-average ratio and *APD* characteristics for the band-limited DS and DP signals. *APD* characteristics are labeled RAYL for Rayleigh-distributed amplitudes or RP for resolved pulses. More specifically, RP designates a step-like *APD* whose amplitude falls below the average power of the VSA noise at least 10% of the time. Notice that measured *P/A*s of the DS signals were 0 – 3 dB less than *P/A* of GN-01.

Table 5. Measured Amplitude Characteristics of DP and DS Signals Band-Limited to B_{DTV}

Type	Index	*P/A* (dB)	*APD*
DP	01	23.5	RP
	02	13.8	RP
	03	5.4	
	04	8.1	
DS	01	9.5	RAYL
	02	9.0	RAYL
	03	8.1	
	04	6.6	
	05	6.6	
	06	6.8	
GN	01	9.6	RAYL

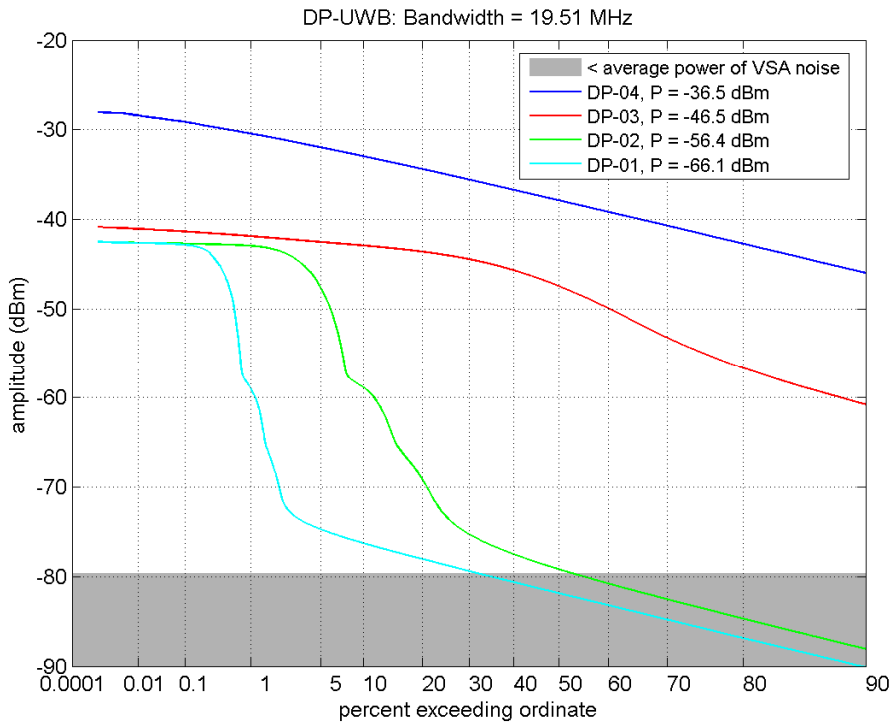

Figure 17. *APD*s of DP signals band-limited to B_{DTV}.

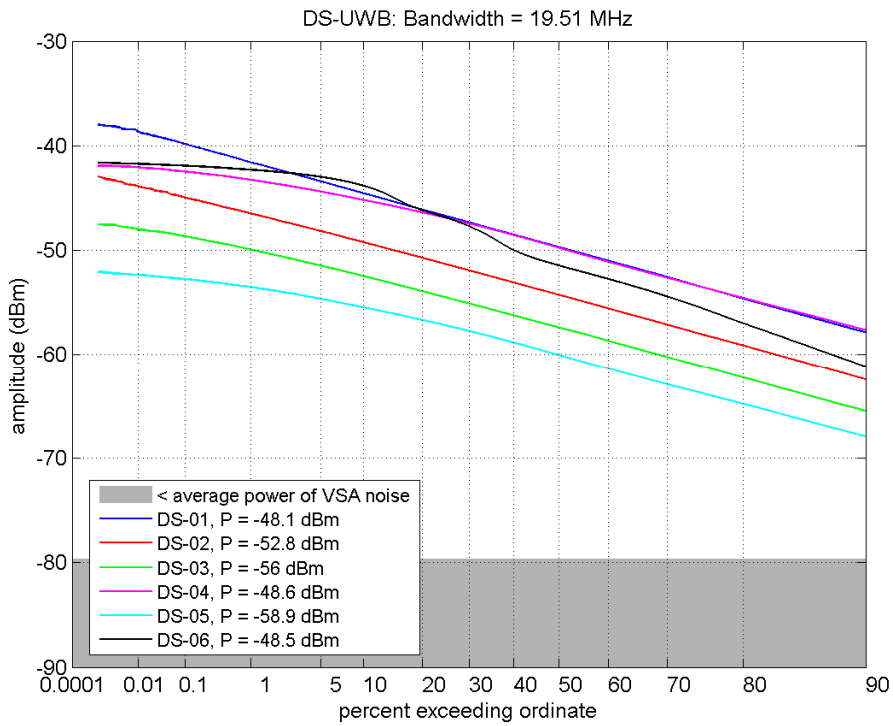

Figure 18. *APD*s of DS signals band-limited to B_{DTV}.

2.3.3. Spectral Analysis

Spectral characteristics of the DP and DS signals were characterized with the power spectral density, which represents the average power present per unit bandwidth as a function of frequency. Appendix A provides theoretical analyses of the *PSD* for DP and DS signals. In short, *PSD*s of the DP signals have discrete and continuous components that depend on the pulse spectrum and the dither function, while *PSD*s of the DS signals have only a continuous component that depends on the pulse spectrum and the code word spectrum.

*PSD*s were calculated from VSA measurements by averaging squared spectrum magnitudes of 500 rectangular-windowed, non-overlapping blocks of signal data. The periodic nature of the signals required that the block size be an integer multiple of the pulse period. To have the same Δf, the block size must also be a common integer multiple of all pulse periods. For the DP signals, these requirements were satisfied with a block size equal to 100 µs, which corresponds to Δf = 10.0 kHz. For the DS signals, these requirements were satisfied with a block size equal to 90.9 µs, which corresponds to Δf = 11.0 kHz.

Figures 19 – 20 provide *PSD*s of the DP and DS signals, respectively, in the frequency band of the DTV victim receiver, i.e., 0 Hz on the plots corresponds to 3820 MHz. The victim receiver RRC filter was not applied to the data in post-measurement processing. The measured *PSD*s of DP signals, DS-01, DS-02, DS-03, DS-04, and DS-05 were flat over the DTV frequency band. In contrast and in agreement with Figure A-6, the *PSD* of DS-06 was not flat due to the code word spectrum. Notice that the measured power densities of the DP and DS signals were proportional to ζ. Also, the spectral line at 0 Hz, most prevalent in DP-01, was due to VSG local-oscillator feed-through. The influence of the VSG local-oscillator feed-through on test results was discussed in Appendix C of Part 1 of this report series.

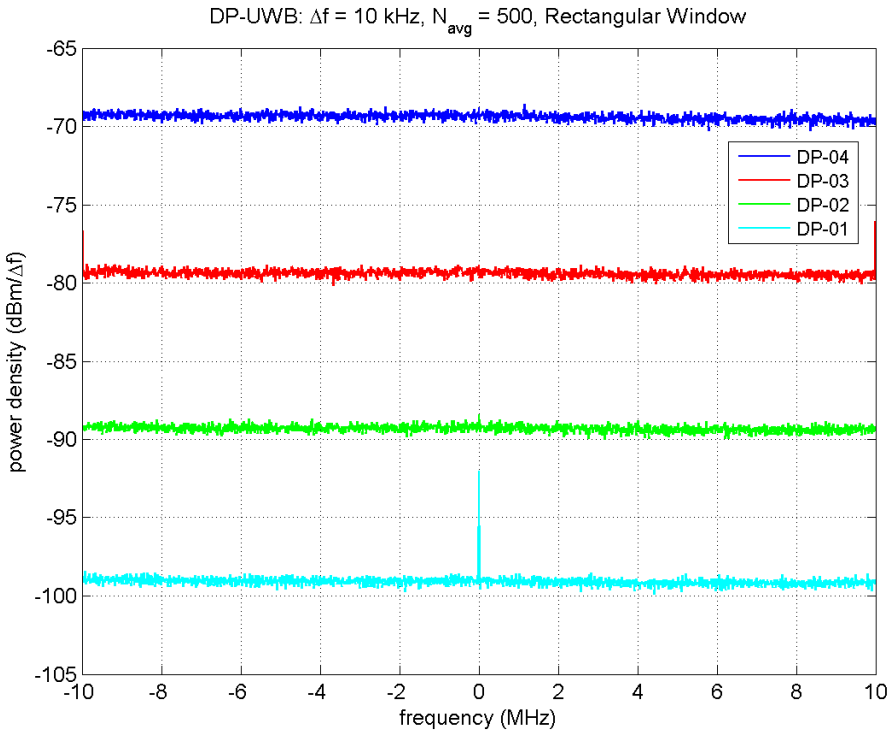

Figure 19. *PSD*s of DP signals.

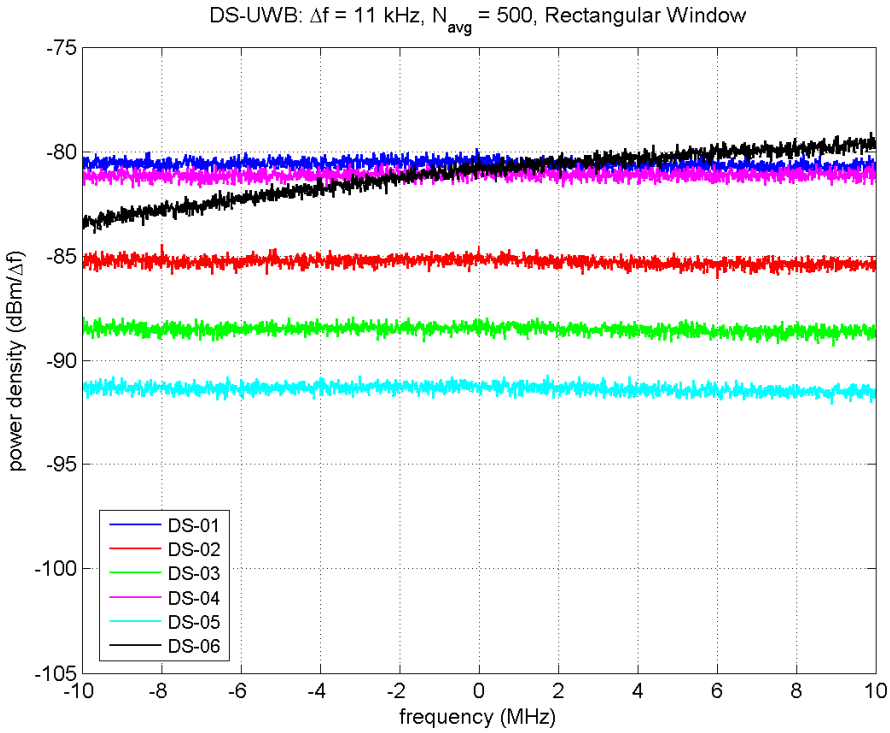

Figure 20. *PSD*s of DS signals.